Localization-delocalization transition of electrons at the percolation threshold of semiconductor GaAs_{1−x}N_{x} alloys: The appearance of a mobility edge

K. Alberi, B. Fluegel, D. A. Beaton, A. J. Ptak, and A. Mascarenhas

Phys. Rev. B **86**, 041201 — Published 9 July 2012

DOI: 10.1103/PhysRevB.86.041201

Localization-delocalization transition of electrons at the percolation threshold of semiconductor $GaAs_{1-x}N_x$ alloys: The appearance of a mobility edge

K. Alberi, B. Fluegel, D.A. Beaton, A.J. Ptak, A. Mascarenhas*

National Renewable Energy Laboratory, Golden CO 80401

Electrons in semiconductor alloys have generally been described in terms of Bloch states that evolve from constructive interference of electron waves scattering from perfectly periodic potentials, despite the loss of structural periodicity that occurs on alloying. Using the semiconductor alloy $GaAs_{1-x}N_x$ as a prototype, we demonstrate a localized to delocalized transition of the electronic states at a percolation threshold, the emergence of a mobility edge, and the onset of an abrupt perturbation to the host GaAs electronic structure, shedding new light on the evolution of electronic structure in these abnormal alloys.

Alloying binary semiconductors is an effective way to tailor electronic properties such as band gaps to values unachievable with the constituents themselves. For conventional alloys, the dependence of the band gap on alloy composition fits a simple quadratic form, where a small bowing parameter is used to account for the deviation from a linear interpolation between the binaries. Recently, a class of isoelectronic alloys have been studied that exhibit a giant band gap bowing together with abnormalities in transport parameters.[1-4] As these alloys offer features highly desirable for photovoltaic and laser devices, there has been significant effort to decipher the mechanisms underlying their abnormal behavior. We now present direct experimental evidence for the effects of Anderson localization on the host band structure and the formation of a mobility edge in these materials, shedding light for the first time on the birth of these abnormal alloys.

Isoelectronic semiconductor alloys such as $GaAs_{1-x}N_x$ that have strong disorder associated with fluctuations in the alloy potentials on the anion sublattice, are known to exhibit a giant band gap bowing and a sharp degradation of the electron mobility, and modifications to the electron effective mass in the dilute alloy regime.[1-4] In dilute $GaAs_{1-x}N_x$ alloys, the bound states generated by N pairs and clusters evolve into impurity bands that broaden and merge with the conduction band edge.[5] Thus in the dilute regime, there exists an enigma as to whether the incorporation of isoelectronic N atoms substitutionally on the anion lattice should be viewed as forming an alloy or as a heavily doped semiconductor.[6] Using optical spectroscopic measurements to probe the evolution of electronic states in the presence of disorder, we provide direct evidence for a localized to delocalized transition, the onset of a mobility edge, and the transformation from a heavy isoelectronically doped semiconductor to the $GaAs_{1-x}N_x$ alloy.[7,8]

$GaAs_{1-x}N_x$ samples with N concentrations < 0.04% were grown by low pressure metal organic chemical vapor deposition with thicknesses of ~ 1 μm. The compositions were confirmed with secondary mass ion spectrometry. Those with N concentrations ≥ 0.04% were grown by molecular beam epitaxy to thicknesses ~ 300 nm, and the compositions were determined by X-ray diffraction. Further details of the growths can be found in Refs. 9,10. Electromodulated reflectance (ER) was measured at 80K as detailed in Ref. 11. ER spectra of the direct band gap transition E_0 associated with the Γ point in the bandstructure and the E_1 and $E_1 + \Delta_1$ transitions associated with the L point are shown in Fig. 1. These spectra are modeled with the third-derivative functional form of Aspnes to extract the critical point energies and linewidth broadening parameter Γ.[12] A plot of Γ as a function of N composition is shown in Fig. 2. At roughly 0.4% N composition the onset of a rapid enhancement in the linewidth broadening of E_0 occurs concomitantly with an enhancement in the broadening of E_1. In contrast, the linewidth broadening of E_0 and E_1 for the conventional semiconductor alloy $In_xGa_{1-x}As$, also shown in Fig. 2, exhibits barely any increase in this dilute composition regime.

To investigate the peculiar sudden enhancement of the linewidth broadening of E_0, photoluminescence (PL) spectra for the $GaAs_{1-x}N_x$ samples were measured at 80K with a 532 nm laser and are shown in Fig. 3. An abrupt change in the character of the PL spectrum appears at N compositions between 0.12% and 0.23%. As the N composition increases above 0.12%, the PL peak A originating from the dominant band edge transition in samples with low N compositions rapidly transitions into a high energy shoulder (peak B) of a broad band (peak C) that has a prominent low energy tail. The red arrows indicate the energy of the E_0 transition measured by ER at 80K for each sample. With an increase in the N composition to 0.12%, the direct band

edge indicated by the red arrow sweeps downward from higher energies until it coincides with PL peak *A*. On further increasing the N composition to 0.23%, the dominant PL from peak *A* is abruptly replaced by that from peak *B* which is separated from the E_0 transition (red arrow). Increasing the N composition beyond 0.23% leads to a convergence of peak *B* with the E_0 transition.

While the isolated N impurity state is resonant with the GaAs conduction band, N pairs and clusters form bound states that constitute a broad peak *C*.[5] The large number of non-equivalent spatial configurations for large size clusters together with strong electron-phonon coupling causes a broadening and smearing out of cluster structure in the PL spectra, leading to the broad continuous band manifested at higher N compositions.[5] N cluster states fall into two categories, localized or delocalized. Because the density of cluster states decreases exponentially with increasing binding energy of the cluster, wavefunction overlap between deep cluster states is minimal.[13,14] These states are spatially isolated and form the low energy tail. For shallow cluster states with smaller binding energies and hence larger localization radii, spatial overlap of their wavefunctions produces superclusters that have finitely extended states. At the percolation threshold for N cluster states, superclusters of infinite size develop with a transition from localized to delocalized states that form peak *B*.[13,14] These different categories of states are revealed in Fig. 3 through the use of an excitation power and lattice temperature chosen to populate a broad spectrum. More selective population of the states can be achieved at lower temperature using pulsed excitation and low average power. Fig. 4 shows time integrated PL spectra measured at 2K for two samples lying on opposite sides of the localized to delocalized transition. Measurements were carried out with a mode-locked Ti:sapphire laser at 2K. Spectral

features corresponding to those of Fig. 3 are labeled here with a primed notation. At low excitation intensity, PL from distinct cluster states that make up *C′* can be identified at lower spectral energies and their evolution into the broad band *C′* (*C* in Fig. 3) on increasing N composition is clearly evident in Fig. 4b. PL decay curves 1-3 shown in the insets correspond to time-resolved PL (TRPL) at 2 K from the spectral regions marked by the horizontal arrows 1-3. The TRPL was measured by exciting near-resonant to E_0 at 1 μJ/cm^2 (5 μW) and detecting the dispersed PL spectrum with a streak camera. The slow (ns) recombination from the tail states in region 1 is a characteristic of N cluster states that behave as isoelectronic traps.[15,16] Because the localization radius of photogenerated carriers trapped at these deep states is small, the influence of crystal imperfections on their recombination lifetime is significantly diminished. At high excitation intensities the PL at high spectral energies changes dramatically, with the emergence of a new emission peak *A′(B′)* in Fig. 4a(b) which dominates the spectrum. This occurs because at high excitation intensity the faster (ps) recombination in region 2 occurs preferentially. Photoluminescence excitation spectroscopy (PLE) was measured using a stabilized Ti: sapphire laser and the absorption edge E_0' modeled as in Ref. 17**.** As the PLE spectrum shown in Fig. 4 reflects the density of extended states, the proximity of the PLE absorption edge E_0' to peaks *A′(B′)* combined with their fast decay time indicates that they emanate from the edge of a band of extended states.

The origin of this edge can be identified by examining Fig. 5 which shows how the 80K PL peaks *A(B)* and the ER transition energy E_0 from Fig. 3 vary with N composition. The 2K PL and PLE data, not shown here, follow the same trend. The band edge values measured by ER

have error bars of 2 meV. The E_0 trend reflects the smooth but giant drop in band gap with increasing N composition.[18] The abrupt change from peak *A* to *B* in the PL spectrum noted earlier in Fig. 3, now appears as a discontinuity in the variation of their separation from the E_0 band edge as a function of N composition. As peaks *A* and *B* are associated with delocalized states, the discontinuity occurs because PL peak *A* emanating from delocalized states near the conduction band edge abruptly transforms to PL peaks *B* emanating from a newly formed band edge of delocalized states associated with N superclusters. This band edge *B* of delocalized states has split-off from the band *C* of localized N cluster states in Fig.3 and occurs at the percolation threshold discussed earlier. A mobility edge separates the localized states from the delocalized states and leads to the rapid fall in intensity on the high energy side of the *C´* PL lineshape seen in the low power spectrum of Fig.4b.[8] In Fig. 5, the horizontal lines mark prominent discrete levels, and the bands represent dispersions of cluster state energies reported in the literature that arise from intercenter coupling and variations in the N concentration and cluster configurations.[5] As the N concentration increases from 0% to 0.12% the conduction band edge (denoted by E_0) sweeps downward through a series of N cluster localized levels, sequentially engulfing and hybridizing with their electronic states. At 0.23% N concentration, Fig. 3 shows that the conduction band edge E_0 still lies above the newly formed PL peak *B*, but as the N concentration is increased further, E_0 sweeps downwards in energy until at 0.41% N it has overlapped the supercluster emission.[6,19] It is precisely near this composition (see dotted vertical line in Fig. 5) that the abrupt increase in linewidth broadening of the E_0 and E_1 transitions occurs in Fig. 2. The E_1 broadening results from Γ-*L* mixing induced by the N impurity potential.[20] The small blue shift in $E_L = L_c - \Gamma_v$ obtained from the E_1 values through the procedure discussed in Ref. 11 and shown in Fig. 5 results from this mixing. From this composition onwards, the overlap of E_0 with

B, results in the dramatic increase in linewidths of the Γ and *L* critical points signaling the birth of the $GaAs_{1-x}N_x$ alloy.

N impurity pairs/clusters generate bound states in the gap just as donors and acceptors do in GaAs, and heavy *n* or *p*-type doping causes a band-gap reduction as a consequence of impurity band formation analogous to the present situation with isoelectronic impurity doping.[18] This begs the question whether dilute $GaAs_{1-x}N_x$ should be referred to as an alloy or as a heavy isoelectronically doped semiconductor. Evidence for cluster-induced effects on the electronic structure of $GaAs_{1-x}N_x$ implicates impurity bands with the abnormalities in the electronic properties of the alloy.[5,6,21-27] However, theoretical efforts to reconcile these abnormalities have proved to be quite challenging.[19,28,29] Although band gap reduction in $GaAs_{1-x}N_x$ is observed at a mere 0.002% N in Ref. 10, we now observe the occurrence of a crossover from localized to delocalized states between 0.12% and 0.23% N followed by an abrupt enhancement in the linewidth of the Γ and *L* critical point transitions at ≈ 0.4% N. This delineates the regime where $GaAs_{1-x}N_x$ behaves as a heavy isoelectronically doped semiconductor from that where it behaves as an abnormal alloy. Most importantly, this study demonstrates the viability of the isoelectronically doped regime for Anderson localization studies without the complexities of electron-electron interactions encountered in doped semiconductors like Si:P.[7]

Acknowledgments: Research supported by the U.S. Department of Energy, Basic Energy Sciences, Materials Sciences and Engineering Division under DE-AC36-08GO28308.

*angelo.mascarenhas@nrel.gov

1. J.D. Perkins *et al*., Phys. Rev. Lett. **82**, 3312 (1999).

2. N. Mori, K. Hiejima, A. Kubo, A. Patane, L. Eaves, AIP Conf. Proc. **1399**, 23 (2011).

3. W. Shan *et al*., Phys. Rev. Lett. **82**,1221 (1999).

4. R. Mouilet *et al*., Solid State Comm. **126**, 333 (2003).

5. Y. Zhang, A. Mascarenhas, J.F. Geisz, H.P. Xin, C.W. Tu, Phys. Rev. B **63**, 085205 (2001).

6. Y. Zhang *et al*., Phys. Stat. Sol. (b) **240**, 396 (2003).

7. R.C. Dynes, P.A. Lee, Science **223**, 355 **(**1984).

8. N. Mott, Proc. R. Soc. Lond. A **382***,* 1 (1982).

9. A.J. Ptak, S.W. Johnston, S. Kurtz, D.J. Friedman, W.K. Metzger, J. Cryst.Growth **251**, 392 (2003).

10. Y. Zhang *et al.,* Phys. Rev. B **68**, 075210 (2003).

11. S. Francoeur *et al.,* Phys. Rev. B **68**, 075207 (2003).

12. D.E. Aspnes, Surf. Sci. **37**, 418 (1973).

13. A.L. Efros, Sov. Phys. Usp. **21**, 746 (1978).

14. A. Reznitsky, A. Klochikhin, S. Permogorov, in *Spectroscopy of Systems with Spatially Confined Structures*, edited by B. Di Bartolo, Kluwer Academic, Dordrecht, 2003).

15. X. Liu, M.-E. Pistol, L. Samuelson, Phys. Rev. B **42**, 7504 (1990).

16. X.D. Luo *et al.,* Appl. Phys. Lett. **82**, 1697 (2003).

17. R.J. Elliott, Phys. Rev. **108**, 1384 (1957).

18. Y. Zhang, A. Mascarenhas, H.P. Xin, C.W. Tu, Phys. Rev. B **63**, 161303(R) (2001).

19 P.R.C.Kent, A. Zunger, Phys. Rev. Lett. **86**, 2613 (2001).

20 A. Mascarenhas *et al*. Phys. Rev. B **68**, 233201 (2003).

21. P.J. Klar *et al.,* Appl. Phys. Lett. **76**, 3439 (2000).

22. G. Bentoumi *et al.,* Phys. Rev. B **70**, 035315 (2004).

23. J. Endicott *et al*., Phys. Rev. Lett. **91**, 126802 (2003).

24. G. Pettinari *et al*., Phys. Rev. Lett. **98**, 146402 (2007).

25. F. Masia *et al.,* Appl. Phys. Lett. **82**, 4474 (2003).

26. J. Teubert *et al.,* Appl. Phys. Lett. **84**, 747 (2004).

27. F. Ishikawa *et al*., Appl. Phys. Lett. **87**, 262112 (2005).

28. A. Lindsay, E.P. O'Reilly, Phys. Rev. Lett. **93**, 196402 (2004).

29. H.X. Deng *et al*., Phys. Rev. B **82**, 193204 (2010).

Figure Captions

Fig. 1 (Color online). ER spectra in $GaAs_{1-x}N_x$ samples as a function of N composition. Both the E_0 transition (left) and the E_1 and $E_1 + \Delta_1$ transitions (right) are shown. A representative example of a lineshape fit (dashed curve) is shown for the E_0 transition of the 0.12% N sample.

Fig. 2 (Color online). Increase in the broadening of the E_0 and E_1 ER transitions of $GaAs_{1-x}N_x$. The broadening parameters, Γ, are normalized to their respective values in GaAs. Solid lines are a guide to the eye. Normalized values for $Ga_{1-x}In_xAs$ are also shown.

Fig. 3 (Color online). PL spectra of a selected set of $GaAs_{1-x}N_x$ samples measured at 80K. The red arrows indicate the energy of the E_0 transition measured by ER for each sample.

Fig. 4 (Color online). PL, PLE and TRPL spectra for $GaAs_{1-x}N_x$ samples. Time integrated PL spectra for samples with (a) 0.12% N and (b) 0.32% N measured at 1.7 K using femtosecond pulsed laser excitation with power densities of 5 μW and 100 μW. The PL decay curves 1-3 in the insets were measured in the spectral regions marked by the horizontal arrows 1-3. The arrows on the PLE curves denote the absorption edge energy E_0'.

Fig. 5 (Color online). Band edge and PL energies in $GaAs_{1-x}N_x$ as a function of composition. The E_0 (filled squares) and $E_L = L_c - \Gamma_v$ (open squares) transitions measured by ER as in Ref.11. Energies of PL peaks *A/B* in Fig. 3 are shown as open downward-pointing triangles. The composition where the ER broadening increases for the E_0 transition in Fig. 2 is marked with a dotted vertical line. Horizontal lines and bands mark the relative energies of the isolated N and N-cluster states. The Γ and L conduction band edge energies relative to the valence band maximum in GaAs are marked by the arrows on the left.

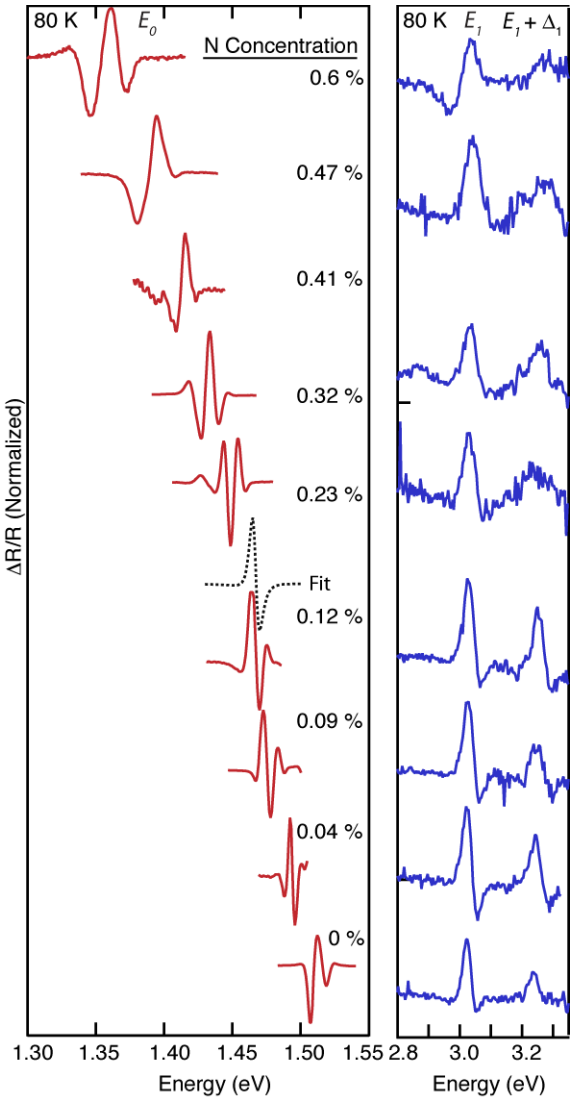
80 K
E_0
N Concentration
0.6 %
0.47 %
0.41 %
0.32 %
0.23 %
Fit
0.12 %
0.09 %
0.04 %
0 %
ΔR/R (Normalized)
1.30 1.35 1.40 1.45 1.50 1.55
Energy (eV)
80 K
E_1
$E_1 + \Delta_1$
2.8 3.0 3.2
Energy (eV)

Figure 1

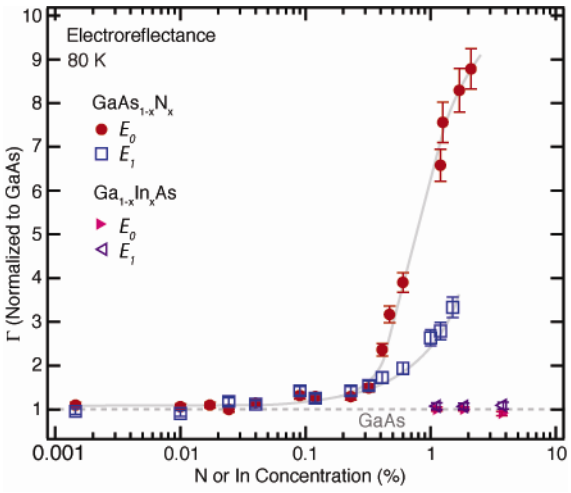
Electroreflectance
80 K
GaAs1-xNx
E0
E1
Ga1-xInxAs
E0
E1
GaAs
Γ (Normalized to GaAs)
N or In Concentration (%)
0.001
0.01
0.1
1
10
1
2
3
4
5
6
7
8
9
10

Figure 2

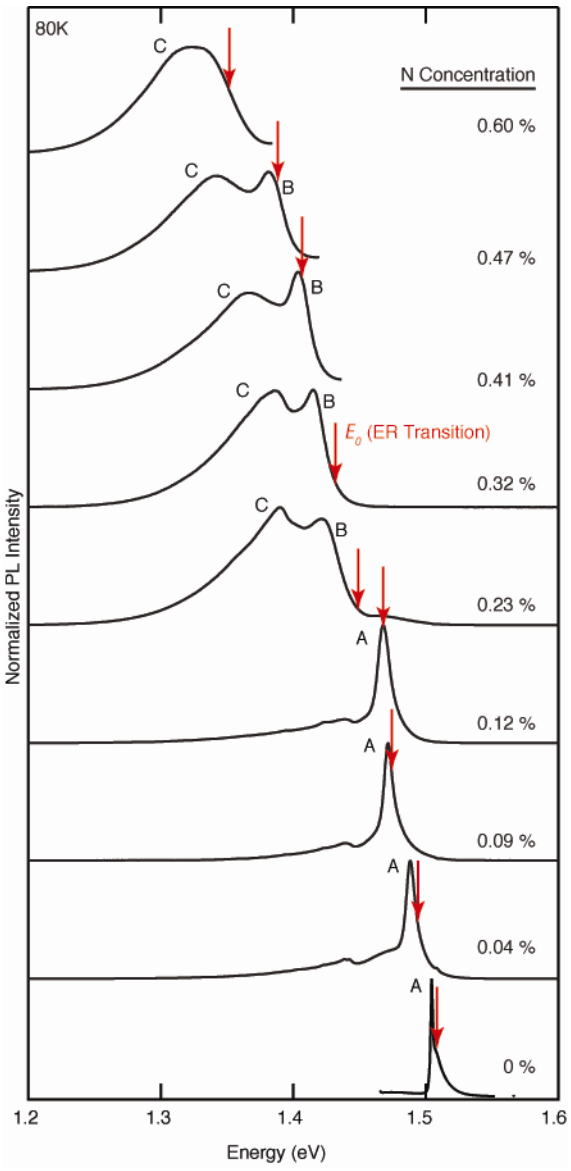
80K
N Concentration
0.60 %
0.47 %
0.41 %
0.32 %
0.23 %
0.12 %
0.09 %
0.04 %
0 %
A
B
C
E_0 (ER Transition)
Normalized PL Intensity
Energy (eV)
1.2
1.3
1.4
1.5
1.6

Figure 3

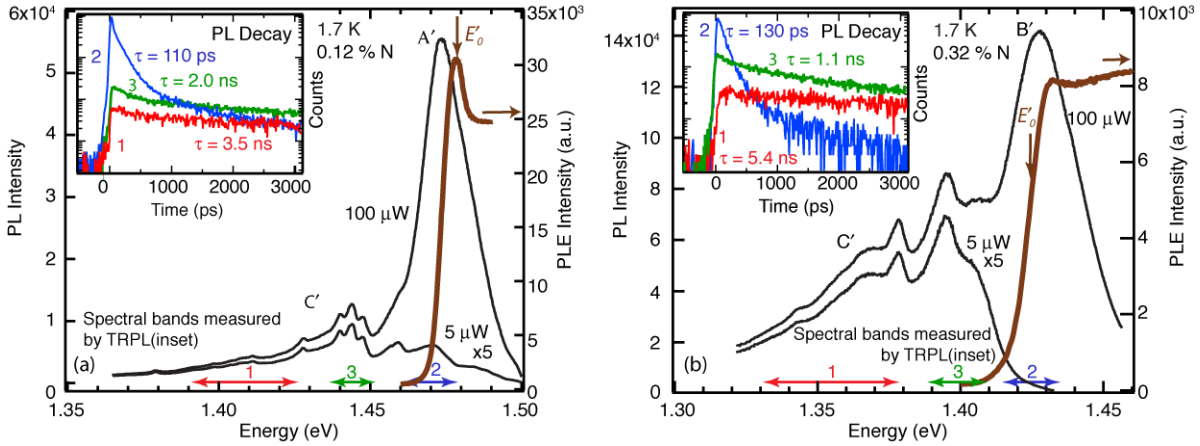

Figure 4

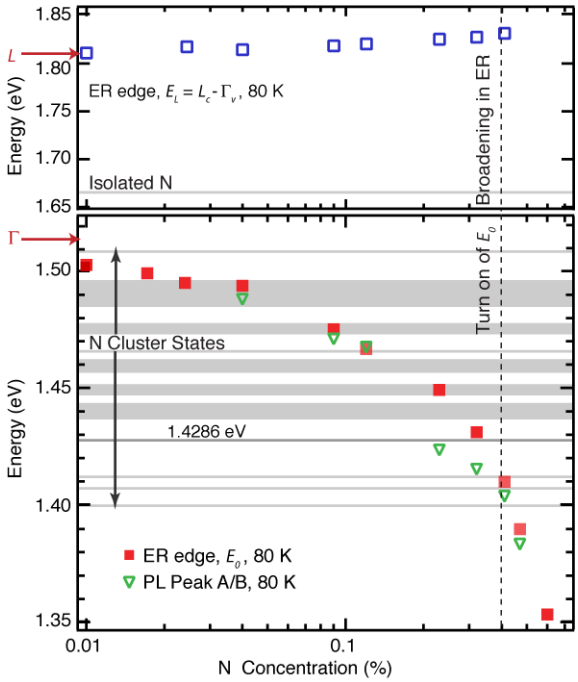

Figure 5